CHIN. PHYS. LETT. Vol. 38, No. 5 (2021) 055202

Observation of Multiple Broadband Alfvénic Chirping Modes in HL-2A NBI Plasmas

Liming Yu(于利明)[1], Wei Chen(陈伟)[1*], Xiaoquan Ji(季小全)[1], Peiwan Shi(施培万)[2], Xuantong Ding(丁玄同)[1], Zhongbing Shi(石中兵)[1], Ruirui Ma(马瑞瑞)[1], Yumei Hou(侯玉梅)[1], Yonggao Li(李永高)[1], Jiaxian Li(李佳鲜)[1], Jianyong Cao(曹建勇)[1], Wulyu Zhong(钟武律)[1], Min Xu(许敏)[1], and Xuru Duan(段旭如)[1]

[1]*Southwestern Institute of Physics, Chengdu 610041, China*
[2]*Key Laboratory of Materials Modification by Laser, Ion and Electron Beams (Ministry of Education), School of Physics, Dalian University of Technology, Dalian 116024, China*

(Received 14 January 2021; accepted 9 March 2021; published online 2 May 2021)

Multiple broadband Alfvénic chirping modes (CMs), with frequencies in the wide range of $f \sim 35$–$150\,\mathrm{kHz}$ and chirping down rapidly, are found in HL-2A neutral beam injection plasmas, and the CMs can even coexist. The frequency chirping down process can be completed within $\sim 1\,\mathrm{ms}$, and the frequency shift can reach 30–50 kHz. The CMs propagate in ion diamagnetic drift directions poloidally. The toroidal mode number is confirmed to be $n = 1$, 2, 3 and 4 for the $f \sim 35$–65, 55–90, 70–120 and 100–150 kHz CMs, respectively. The CMs are more like to be energetic-particle continuum modes (EPMs), since the modes almost locate on the Alfvén continuum.

DOI: 10.1088/0256-307X/38/5/055202

Energetic particles (EPs), which are generated by auxiliary heating and deuterium-tritium (D-T) fusion reactions, will excite various magnetohydrodynamic (MHD) instabilities,[1−7] such as energetic-particle continuum mode (EPM), beta-induced Alfvén eigenmode (BAE), toroidal Alfvén eigenmode (TAE), reversed shear Alfvén eigenmode (RSAE), and elongation Alfvén eigenmode (EAE). However, a serious loss and redistribution of EPs can be caused by the MHD instabilities. The first wall can even be destroyed by the abundant loss of EPs.[8] The effects of Alfvén eigenmodes on the loss and distribution of EPs in burning plasmas are predicted by simulation.[9] Meanwhile, MHD instabilities are excepted to be a channel to expel the helium (He) ash and to transfer energy and momentum of EPs to background plasma. In addition, the valuable information of plasma parameters can be offered by the characteristics of MHD instabilities. Therefore, understanding the behavior and effect of MHD instabilities driven by EPs are very important.

According to the theory of general fishbone-like dispersion relationship (GFLDR)[10,11] set up by Zonca and Chen, the EPs-induced MHD instabilities can be divided into two categories: (1) discrete gap modes and (2) EPMs. The discrete gap modes, such as BAE, TAE, RSAE, and EAE, locate on the gap of Alfvén continuum and suffer from weak damping. The behaviors of the discrete gap modes strongly depend on the equilibrium parameters. The EPMs, including fishbone mode and the high-frequency Afvénic chirping modes (CMs), can be driven by the EPs directly because the abundant EPs can overcome the Alfvén continuum damping. The frequencies of the EPMs are determined by the characteristic frequencies of EPs, e.g., transit (ω_t), bounce (ω_b), precessional (ω_p) and even their combination ($\omega = n\omega_\mathrm{p} \pm l\omega_\mathrm{t,b}$), where n is the toroidal mode number, $l = 1, 2, \ldots$ For most time, the frequencies of the EPMs chirp down rapidly.

The fishbone mode, which is explained to resonance between internal kink mode and characteristic motions of EPs, has been observed and studied in many tokamaks in experiment[12−15] and theory.[16,17] The high-frequency EPMs, with $f \sim 20$–$150\,\mathrm{kHz}$, are observed on DIII-D,[18] JT-60U,[19] NSTX[20,21] and CHS[22,23] during neutral beam injection (NBI) heating. Serious losses of EPs caused by the CMs are measured.[18−23] The fishbone mode will be excited by the EPs when there is the $q \sim 1$ rational surface,[24] while the high-frequency CMs will be driven when the minimum q (q_min) is larger than unity.[20] Recently, the $f \sim 0$–$8\,\mathrm{kHz}$ off-axis fishbone-like chirping tearing modes (TMs)[25,26] excited by the resonance between TM and energetic ions (EIs) are found on HL-2A. Some phenomena of chirp-down (or up) modes on HL-2A are explained by the hole-clump model[27]

Supported by the National Key R&D Program of China (Grant Nos. 2018YFE0304102, 2019YFE03020000 and 2017YFE0301202), the National Natural Science Foundation of China (Grant Nos. 11875024, 11875021, 11835010 and 12005054), the Sichuan Provincial Science and Technology Project (Grant Nos. 2020YFSY0047 and 2020JDJQ0070).
*Corresponding author. Email: chenw@swip.ac.cn
© 2021 Chinese Physical Society and IOP Publishing Ltd

successfully.

Multiple broadband Alfvénic CMs induced by the EIs have been found in HL-2A NBI plasmas. In this Letter, first, the typical examples and characteristics of the four frequency bands CMs, including the mode frequency, the frequency chirping down processes and identification of mode numbers, are investigated. Then, the Alfvén continuum are calculated based on the common pure NBI heating discharge parameters. The CMs almost locate on the Alfvén continuum. Therefore, the CMs observed on HL-2A are more like to be EPMs. The effects of distribution of EIs and the other key factors on the behaviors of CMs are discussed. Finally, conclusions are given.

Typical Examples and Characteristics of CMs. HL-2A is a medium-sized tokamak with a circular cross section (major radius $R_0 = 1.65\,\mathrm{m}$ and minor radius $a = 0.40\,\mathrm{m}$).[28] The main auxiliary heating systems, including the NBI[29] and electron cyclotron resonant heating (ECRH),[30,31] are used to heat the plasma and generate EPs. The NBI tangentially co-injects into the HL-2A tokamak with an injection angle of 58.1° and a tangency radius of 1.35 m. The energy of the beam particles (E_b) can be accelerated to 40–45 keV. The power of NBI, P_NBI, can reach 1.5 MW. The ECRH system is composed of six 68 GHz/500 kW gyrotrons. The ECRH injects into the plasma from the low-field side with O- or X-mode in the perpendicular direction. The power of ECRH (P_ECRH) at deposited position r (in the minor radius) can be changed by varying the toroidal magnetic field B_t. The relationship between r and B_t satisfies $r = 28NB_\mathrm{t}R_0/f_\mathrm{ECRH} - R_0$, where $N = 2$ (ECRH works in X-mode) and $f_\mathrm{ECRH} = 68\,\mathrm{GHz}$ in our experiments. The P_ECRH will be deposited on the position of $r = 0.20$–$0.25\,\mathrm{m}$ region when B_t is in the range of 1.36–1.40 T in the experiment.

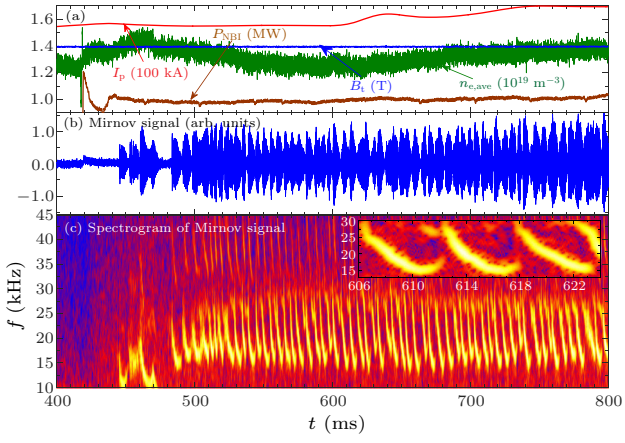

Fig. 1. Typical example of fishbone mode in NBI plasma in shot 19801. (a) Discharge parameters of plasma current (I_p), line-averaged electron density ($n_\mathrm{e,ave}$), P_NBI and B_t, (b) Mirnov signal of poloidal magnetic probe and (c) its spectrogram.

The fishbone mode is a very common low-frequency (10–30 kHz) CM in NBI plasmas on HL-2A. Figure 1 shows an example of the strong fishbone modes. The discharge parameters are $I_\mathrm{p} \sim 150$–$170\,\mathrm{kA}$, $n_\mathrm{e,ave} \sim (1.2\text{–}1.4) \times 10^{19}\,\mathrm{m}^{-3}$, $B_\mathrm{t} = 1.4\,\mathrm{T}$ and $P_\mathrm{NBI} = 1.0\,\mathrm{MW}$, as shown in Fig. 1(a). The strong bursts can be found from the Mirnov signal (Fig. 1(b)) after the injection of NBI. The frequency of fishbone mode chirps down from 30 to 15 kHz within 5–7 ms, as shown in Fig. 1(c). The chirping shift (Δf) and $\Delta f/f$ can reach ∼15 kHz and ∼50%.

Except for the low-frequency fishbone mode, four high-frequency broadband CMs, with frequencies in the range of ∼35–65, 55–90, 70–120 and 100–150 kHz, are found in pure NBI or NBI + ECRH plasmas. The Δf can reach ∼30–50 kHz, and the frequency chirp-down processes of CMs can be completed within ∼1 ms.

There is a typical example of $f \sim 35$–$65\,\mathrm{kHz}$ CMs, as shown in Fig. 2. The discharge parameters are $I_\mathrm{p} \sim 119$–$140\,\mathrm{kA}$, $n_\mathrm{e,ave} \sim (0.7\text{–}0.9) \times 10^{19}\,\mathrm{m}^{-3}$, $B_\mathrm{t} = 1.39\,\mathrm{T}$, $P_\mathrm{NBI} = 1.0\,\mathrm{MW}$ and $P_\mathrm{ECRH} = 0.87\,\mathrm{MW}$, as shown in Fig. 2(a). The obvious fluctuations are found on Mirnov signals after the injection of NBI, as shown in Fig. 2(b). The strong CMs are found on the spectrogram of Mirnov signal, as shown in Fig. 2(c). The mode frequency can chirp down from 65 to 35 kHz within 1 ms. The Δf and $\Delta f/f$ can reach ∼30 kHz and ∼46%.

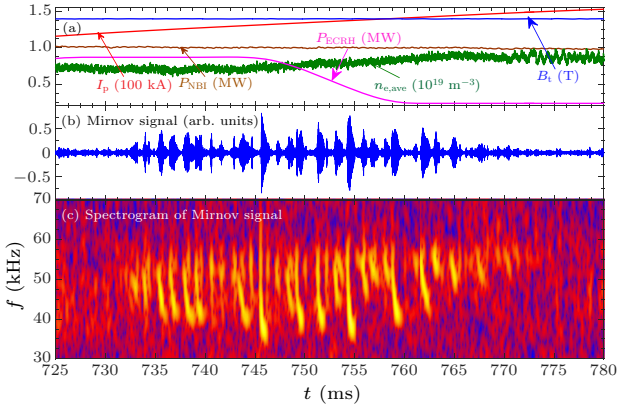

Fig. 2. The 35–65 kHz CMs observed in NBI + ECRH plasma in shot 19051. (a) Discharge parameters, (b) Mirnov signal of poloidal magnetic probe and (c) its spectrogram.

Two frequency bands (55–90 and 70–120 kHz) CMs are found in NBI + ECRH and NBI plasmas in shot 18994. The discharge parameters are $I_\mathrm{p} \sim 153$–$160\,\mathrm{kA}$, $n_\mathrm{e,ave} \sim (1.2\text{–}2.0) \times 10^{19}\,\mathrm{m}^{-3}$ and $B_\mathrm{t} = 1.38\,\mathrm{T}$, as shown in Fig. 3(a). Although the 1.1–1.3 MW ECRH switches on first, the CMs are not found until the injection of 1.0 MW NBI. The clear frequency chirp-down process of 55–90 kHz CMs can be found in the spectrogram of Mirnov signal in Fig. 3(c1), and the

Δf and $\Delta f/f$ can reach ∼30 kHz and ∼33%. Except that, the $f \sim$ 70–120 kHz CMs, with $\Delta f \sim$ 50 kHz and $\Delta f/f \sim$ 42%, are found when ECRH are turned off and only NBI heating at $t =$ 900–970 ms. There is a clear segment of 70–120 kHz CMs during $t =$ 930–955 ms, as shown in Fig. 3(c2).

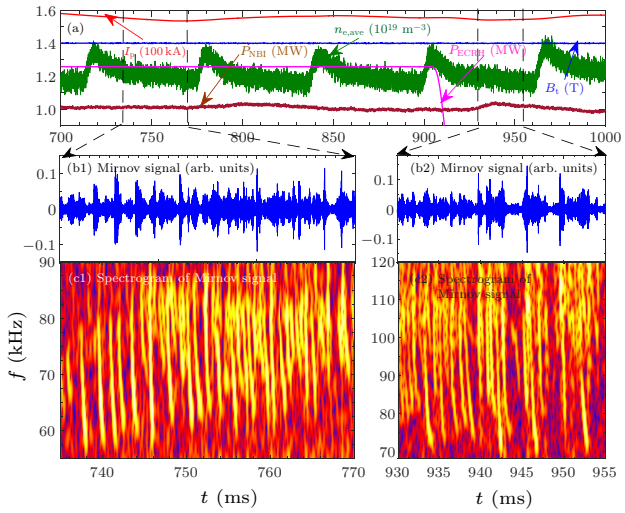

Fig. 3. The 55–90 and 70–120 kHz CMs observed in NBI + ECRH and NBI plasma in shot 18994. (a) Discharge parameters, ((b1), (b2)) Mirnov signal of poloidal magnetic probe, ((c1), (c2)) spectrogram of Mirnov signal during different time periods.

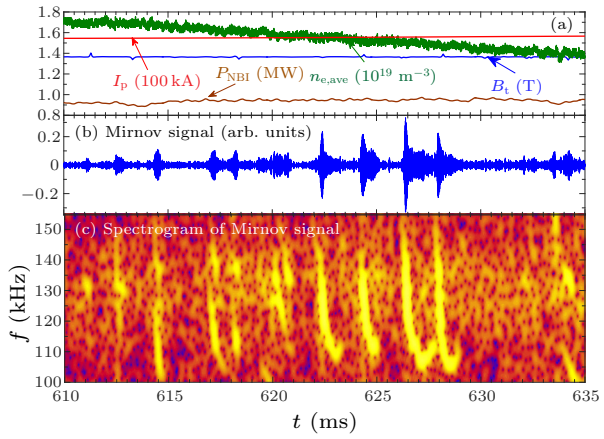

Fig. 4. The 100–150 kHz CMs observed in NBI plasma in shot 21714. (a) Discharge parameters, (b) Mirnov signal of poloidal magnetic probe and (c) its spectrogram.

The $f \sim$ 100–150 kHz CMs are also found in the NBI plasmas in shot 21741, as shown in Fig. 4. The discharge parameters are $I_p \sim$ 155 kA, $n_{e,ave} \sim (1.4–1.7) \times 10^{19}$ m^{-3} and $B_t =$ 1.37 T. The 100–150 kHz strong CMs are found in the spectrogram of Mirnov signal when the 0.9 MW NBI injects into the plasma.

According to the empirical experiment observation, there are four broadband CMs. The left-hand panels (a1)–(d1) in Fig. 5 are the four selected strong and clear frequency chirp-down segments (with time interval of 20 ms) of the above CMs shown in Fig. 2(c), Figs. 3(c1) and (c2), and Fig. 4(c), respectively. The corresponding toroidal mode numbers are confirmed as $n =$ 1, 2, 3 and 4 for the four frequency bands ($f \sim$ 35–65, 55–85, 70–120 and 110–150 kHz) CMs by the phase shift of the filtered toroidal Mirnov probe waveform arrays, as shown in the right-hand panels (a2)–(d2) in Fig. 5. It seems that the higher the frequencies of CMs are, the larger the toroidal mode number is. The poloidal mode number m is difficult to identify, but the ion diamagnetic drift direction of the four CMs can be confirmed by the phase shift direction of the filtered poloidal Mirnov signal arrays.

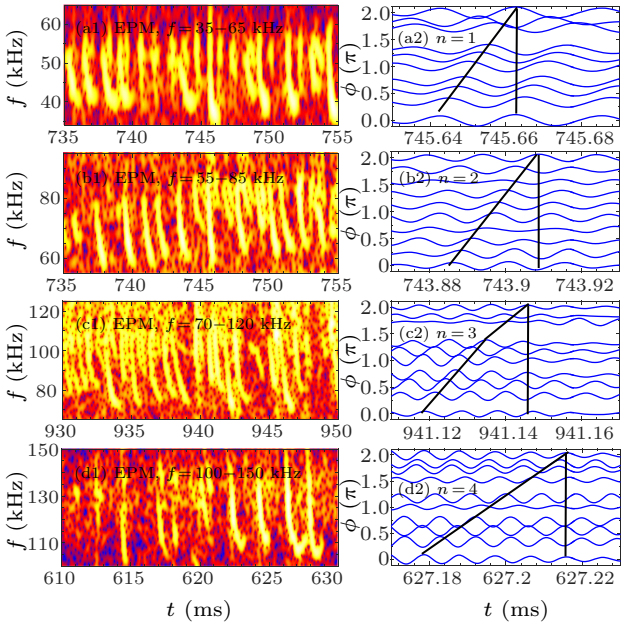

Fig. 5. (a1)–(d1) The typical examples of CMs with frequencies in the range of 35–65, 55–85, 70–120 and 100–150 kHz found from spectrogram of Mirnov signal in NBI or NBI + ECRH plasmas. (a2)–(d2) The toroidal mode number of the CMs confirmed by the phase shift method.

Table 1. Experimental discharge parameters and features of the CMs on HL-2A. Here two columns of shot 18994 correspond to different times and different P_{ECRH}.

Shot	19051	18994	18994	21714	34552
I_p (kA)	120–150	154–160	154–160	155	155
$n_{e,ave}$ (10^{19}/m^3)	0.7–0.9	1.2–1.4	1.2–1.4	1.4–1.7	1.6–1.8
B_t (T)	1.39	1.38	1.38	1.37	1.36
P_{NBI} (MW)	1.0	1.0	1.0	0.9	0.7
P_{ECRH} (MW)	0.87	1.3	0.0	0.0	0.0
f (kHz)	35–65	50–90	70–120	100–150	60–150
Δf (kHz)	30	30	50	50	
Δt (ms)	≤ 1	≤ 1	≤ 1	≤ 1	≤ 1
n	1	2	3	4	1–4
Mode	CM_1	CM_2	CM_3	CM_4	CM_{1-4}

The experimental discharge parameters and features of the the above typical CMs examples and the new found coexistence of four branches CMs as shown in Figs. 2–4 and Fig. 6 are listed in Table 1.

Furthermore, coexistence of four branches CMs

are found in NBI plasma in shot 34552, as shown in Fig. 6. The discharge parameters are $I_p \sim 155$ kA, $n_{e,ave} \sim (1.6\text{–}1.8)\times10^{19}$ m^{-3}, $B_t = 1.36$ T and $P_{NBI} = 0.7$ MW, as shown Fig. 6(a). The frequencies of the CMs are in the wide range of 60–150 kHz. The frequencies of the four branch CMs are in the range of 60–80, 70–100, 95–125 and 100–150 kHz, respectively. There are a lot of overlaps in frequency between the adjacent branch CMs. The toroidal mode numbers for the four co-existing CMs are $n = 1$, 2, 3 and 4, which are labeled on Fig. 6(c). The multi-mode CMs, with different mode numbers, different frequencies and wave lengths, may cause more serious loss of EIs and degradation of confinement than a single mode.

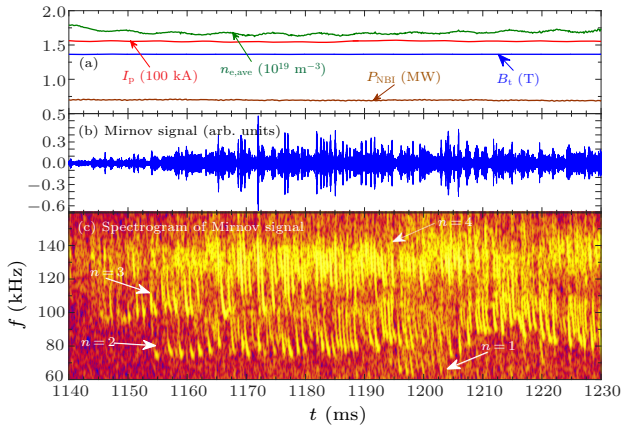

Fig. 6. Strong multi-mode CMs in NBI plasma in shot 34552. (a) Discharge parameters, (b) Mirnov signal from poloidal magnetic probe and (c) its spectrogram.

Analysis and Discussion. The common pure NBI heating discharge parameters, such as electron density (n_e) profile (green curve), electron and ion temperature (T_e and T_i) profiles (purple and red curves) and q profile (black curves), on HL-2A are presented in Figs. 7(a) and 7(b), respectively. The Alfvén continuum with $n = 4$ and $m = 1$–25 are calculated by the AWCON code[32] according to the discharge parameters as mentioned above. The purple- and blue-dashed curves are the TAE frequency (f_{TAE}) and the continuum accumulation point frequency of BAE ($f_{BAE-cap}$). The expressions of f_{TAE} and $f_{BAE-cap}$ are presented as $f_{TAE} = \frac{B_t}{4\pi q R_0\sqrt{\mu_0 n_i m_i}}$ and $f_{BAE-cap} = \frac{1}{\pi R}\sqrt{\frac{T_i}{2m_i}}\sqrt{\frac{7}{4}+\frac{T_e}{T_i}}$, respectively. The CMs are confirmed to be at the core of plasma (near or inside $q = 2$ surface) in experiment, roughly. Usually, the frequency of BAE (f_{BAE}) and TAE are in the ranges of 30–60 kHz and 120–150 kHz in experiment. The 60–120 kHz CMs mostly locate on the Alfvén continuum, and can be identified as typical EPMs. Although the 35–65 and 100–150 kHz CMs partly locate on the BAE and TAE gaps, and their frequencies are close to $f_{BAE-cap}$ and f_{TAE}, the CMs have the typical characteristics of EPMs, such as rapid frequency chirping down behaviors. Therefore, the multiple broadband Alfvénic CMs in NBI plasmas on HL-2A tokamak are more like to be EPMs.

Because the EPMs are driven by the strong pressure of EPs directly, the distribution and energy of EPs are strongly related with the behaviors of EPMs, such as mode structures and frequencies. According to the injection direction of the NBI system on HL-2A, the EPs are dominated by the circulating EIs. Some MHD instabilities on HL-2A are proven to be excited by the circulating EIs. For example, the fishbone mode[33] and fishbone-like chirping TM[26] are confirmed theoretically to be in resonance between the circulating EIs and the corresponding internal kink mode and TM. The transit frequency ($\omega_t = v_{\|}/(qR)$) and precessional frequency ($\omega_p \propto Eq/(eB_tRr)$) of the deuterium ion ($D^+$), with $E_b = 42$ keV, $v_{\|}/v \sim 0.85$ and $B_t = 1.4$ T, are about 90–130 and 30–70 kHz on the core of plasma ($\rho = r/a = 0.1$–0.5). The frequencies of the most CMs (ω_{CMs}), ω_t and ω_p satisfy the relationships $\omega_{CMs} \sim \omega_t$ and $\omega_{CMs} \sim n\omega_p$. Therefore, the CMs are very likely to be excited by the circulating EIs. Further hybrid simulation will be needed to confirm whether the circulating or trapped EIs excite the CMs.

The injection depth of the neutral beam particles (before ionization) is related with the capture length ($\lambda = 1/(n_e\sigma_{eff})$,[34] where σ_{eff} is the total effect capture cross section). The distribution of EIs strongly depends on the n_e profile. Then, the EIs will be slowed down because of collision with the background plasmas. The slowing-down time of EIs (τ_s) is related with the T_e and n_e in the background plasma,[35] that is, $\tau_s \propto T_e^{3/2}/n_e$. The ratio of P_{NBI} deposited on background electrons and ions is determined by the critical energy ($E_{crit} \propto T_e$).[35] If $E_b = E_{crit}$, the energies of EIs transferring to background electrons and ions are equal to each other. If $E_b > E_{crit}$, the electron collisions are dominant. Otherwise, the ion collisions are dominant. In addition, the directional injection of NBI will cause the drive current of NBI (I_b), which is related with the basic discharge parameters n_e, T_e, T_i and so on.[36,37] The ECRH can increase T_e efficiently, and lead to the decrease in n_e by pump-out effect. The q profile will be effected by the value and profile of I_b. Therefore, the ECRH will indirectly affect the q profile.

Although the discharge parameters of some example CMs shots in Table 1 are almost the same, in fact the specific n_e and temperature profiles are quite different. The detail differences of the profiles lead to the great different distributions of EIs and q profile. This is a probably reason why different branch CMs are found under conditions of almost the same dis-

charge parameters. The turn-off of ECRH will lead to the sharp drop of T_e and changes in n_e profile directly. Further, the parameters (e.g., λ, τ_s, E_{crit}, I_b (or q)), which are related with the T_e and n_e, will change obviously. Therefore, the turn-off of ECRH leads to the transition from the 55–90 kHz $n = 2$ CMs to the 70–120 kHz $n = 3$ CMs, as shown in panels (c1) and (c2) of Fig. 3, respectively. The exact reasons of these phenomena need to be further confirmed by more experimental evidence and simulations.

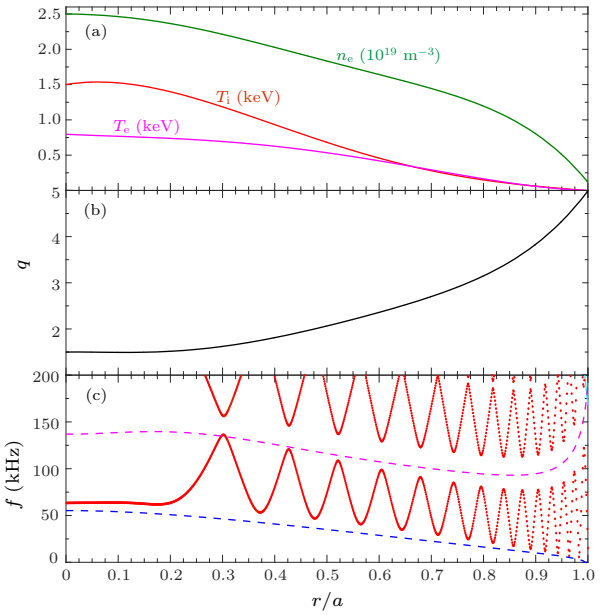

Fig. 7. Alfvén continuum based on the common pure NBI heating discharge parameters on HL-2A. (a) Electron density (n_e) profile, electron and ion temperature (T_e and T_i) profiles, (b) q-profile, and (c) Alfvén continuum with $n = 4$ and $m = 1$–25 calculated by AWCON code.

In summary, the multiple broadband Alfvénic CMs are observed with high-power NBI or NBI + ECRH on HL-2A tokamak. The frequencies of the CMs are in the wide range of $f \sim 35$–150 kHz. The Δf can reach ~30–50 kHz within ~1 ms. All the CMs propagate in ion diamagnetic drift directions poloidally. The toroidal mode numbers for $f \sim 35$–65, 55–90, 70–120 and 100–150 kHz CMs are confirmed as $n = 1$, 2, 3 and 4, respectively. The coexistence of CMs of the four frequency bands are found. The more serious loss of EPs and degradation of confinement may be caused by the multi-mode CMs than a single CM. The high mode frequencies of CMs correspond to the large value of toroidal mode number. The CMs are more like to be EPMs based on the Alfvén continuum calculated from the common NBI heating discharge parameters on HL-2A.

The author (Yu Liming) would like to thank the HL-2A team for tokamak device operation and much technical assistance.

References

[1] Heribrink W W 2002 *Phys. Plasmas* **9** 2113
[2] Chen L 2016 *Rev. Mod. Phys.* **88** 015008
[3] Chen W and Wang Z X 2020 *Chin. Phys. Lett.* **37** 125001
[4] Chen W *et al.* 2016 *Nucl. Fusion* **56** 036018
[5] Qiu Z Y *et al.* 2018 *Phys. Rev. Lett.* **120** 135001
[6] Shi P W *et al.* 2021 *Chin. Phys. Lett.* **38** 035202
[7] Chen W *et al.* 2017 *Nucl. Fusion* **57** 114003
[8] Fasoli A *et al.* 2007 *Nucl. Fusion* **47** S264
[9] Zou Y P *et al.* 2021 *Chin. Phys. Lett.* **38** 045203
[10] Chen L 1994 *Phys. Plasmas* **1** 1519
[11] Zonca F and Chen L 2006 *Plasma Phys. Control. Fusion* **48** 537
[12] MciGuire K *et al.* 1983 *Phys. Rev. Lett.* **50** 891
[13] Heidbrink W W and Sadler G J 1994 *Nucl. Fusion* **34** 535
[14] Chen W *et al.* 2010 *Nucl. Fusion* **50** 084008
[15] Yu L M *et al.* 2017 *J. Phys. Soc. Jpn.* **86** 024501
[16] Chen L, White R B and Rosenbluth M N 1984 *Phys. Rev. Lett.* **52** 1122
[17] Betti R and Freidberg J P 1993 *Phys. Rev. Lett.* **70** 3428
[18] Heidbrink W W 1995 *Plasma Phys. Control. Fusion* **37** 937
[19] Shinohara K *et al.* 2001 *Nucl. Fusion* **41** 603
[20] Fredrickson E *et al.* 2003 *Nucl. Fusion* **43** 1258
[21] Fredrickson E *et al.* 2006 *Phys. Plasmas* **13** 056109
[22] Isobe M *et al.* 2006 *Nucl. Fusion* **46** S918
[23] Nagaka K *et al.* 2008 *Phys. Rev. Lett.* **100** 065005
[24] Zhang R B *et al.* 2014 *Plasma Phys. Control. Fusion* **56** 095007
[25] Chen W *et al.* 2019 *Nucl. Fusion* **59** 096037
[26] Zhu X L *et al.* 2020 *Nucl. Fusion* **60** 046023
[27] Hou Y M *et al.* 2021 *Chin. Phys. Lett.* **38** 045202
[28] Yang Q W *et al.* 2007 *Nucl. Fusion* **47** S635
[29] Wei H L *et al.* 2014 *41st EPS Conference on Plasma Physics* (Berlin, Germany, 23–27 June 2014) p 4.030
[30] Rao J *et al.* 2009 *Nucl. Fusion Plasma Phys.* **29** 324 (in Chinese)
[31] Huang M *et al.* 2010 *37th EPS Conference on Plasma Physics* (Dublin, Ireland, 21–25 June 2010) p 5.166
[32] Deng W *et al.* 2012 *Nucl. Fusion* **52** 043006
[33] Yu L M *et al.* 2019 *Nucl. Fusion* **59** 086016
[34] Yuan B S, Jiang S F and Lu Z H 2011 *Engineering Fundamentals of Tokamak Device* (Beijing: Atomic Energy Press) chap 11 p 413 (in Chinese)
[35] ITER Physics Expert Group on Energetic Particles, Heating and Current Drive and ITER Physics Basis Editors 1999 *Nucl. Fusion* **39** 2471
[36] Wang J 2008 *PhD Dissertation* (Hefei: University of Science and Technology of China) (in Chinese)
[37] Wang J F 2010 *PhD Dissertation* (Hefei: University of Chinese Academy of Sciences) (in Chinese)